Synthesis and cyclic voltammetric properties of $Zn_5(OH)_8Cl_2·H_2O$/PAM composite particles

Q. Y. Huang[a,*], S. Z. Wang[b]

[a]*College of Chemical Engineering, Daqing Normal University, Daqing 163712, China*

[b]*Organic Geochemical Laboratory, Exploration and Development Research Institute of Daqing Oilfield Co Ltd, Daqing 163712, China*

In this study, $Zn_5(OH)_8Cl_2·H_2O$/PAM composite particles (CPs) were synthesized by precipitation reaction and emulsion polymerization in microreactors formed by nano water droplets when the hydrophilic-hydrophilic equilibrium (HLB) value was 5.76. The experimental results showed that $Zn_5(OH)_8Cl_2·H_2O$/PAM CPs were close to the spherical shape with an average diameter of about 736 nm. The CPs contained Zn-O bonds and were covered by PAM. The modified electrode by $Zn_5(OH)_8Cl_2·H_2O$/PAM had good cyclic voltammetry characteristics at scan rate of 100 mVs^{-1} and cyclic potential of +0.8-0.0V, and can detect 0.00001M iodide. In the range of 50-400 mVs^{-1}, the peak current had a linear relationship with the square root of the scan rate and the electrochemical reaction of iodide on $Zn_5(OH)_8Cl_2·H_2O$/PAM/GCE belonged to diffusion control kinetics.

(Received December 14, 2020; Accepted April 3, 2021)

Keywords: $Zn_5(OH)_8Cl_2·H_2O$/PAM CPs, HLB, Modified electrode, Cyclic voltammetric properties

1. Introduction

In recent years, some studies have reported important technical applications of transition metal layered hydroxide materials [1,2], including $Zn_5(OH)_8Cl_2·H_2O$. It is a complex layered zinc chloride hydroxide hydrate with special plate-shaped hexagonal crystal structure. As a wide gap semiconductor material or used for preparing zinc oxide with special structure [3-5], it has been studied and concerned in many aspects recently. For example, Tanaka et al. [6] reported the preparation of $Zn_5(OH)_8Cl_2·H_2O$ powder. Zhang et al. [7] prepared large-size $Zn_5(OH)_8Cl_2·H_2O$ crystal by hydrothermal slow cooling process. Similar to ZnO, $Zn_5(OH)_8Cl_2·H_2O$ contains electrochemical active sites with high efficient charge storage and is suitable for gas sensing [8] and other application fields. $Zn_5(OH)_8Cl_2·H_2O$ combined with graphene can form ultracapacitor materials [9]. With the deepening of research, $Zn_5(OH)_8Cl_2·H_2O$ will be more and more widely applied.

Inorganic and organic composite materials have always been a hot topic of research [10-12], mainly because appropriate changes in the composition, particle size and microstructure of such composite materials will produce some special functions, such as catalytic properties, electrical properties, optical properties or magnetic properties. The composite material organically

* Corresponding author: 5031416@163.com

combines inorganic particles and polymers to achieve mutually beneficial effects, forming a new material with multiple functions.

But up to now, there were few reports on the formation of composite particles between $Zn_5(OH)_8Cl_2·H_2O$ and organic materials. Therefore, in the study, $Zn_5(OH)_8Cl_2·H_2O$/PAM composite particles (CPs) were synthesized in water-in-oil emulsion according to the synthesis mechanism of Fe_3O_4/PAM nano-hydrogel [13]. The synthesis mechanism of $Zn_5(OH)_8Cl_2·H_2O$/PAM CPs was shown in Fig. 1. The $Zn_5(OH)_8Cl_2·H_2O$ CPs were synthesized by precipitation reaction and emulsion polymerization in microreactors formed by nano water droplets.

It was well known that the intake of iodide played an important role in regulating the body function, so it was of great significance for the determination of iodide content [14,15]. Tian et al. [16] used composite glass-carbon electrode (GCE) to determine the iodide content by cyclic voltammetry (CV), and achieved good research results. In the paper, $Zn_5(OH)_8Cl_2·H_2O$/PAM CPs were used to modify GCE to form $Zn_5(OH)_8Cl_2·H_2O$/PAM/GCE. The CV curves for testing iodide of various concentrations on $Zn_5(OH)_8Cl_2·H_2O$/PAM/GCE was obtained, and the electrochemical properties of $Zn_5(OH)_8Cl_2·H_2O$/PAM CPs were studied. It was expected to provide some useful methods for synthesis and research of $Zn_5(OH)_8Cl_2·H_2O$/PAM CPs.

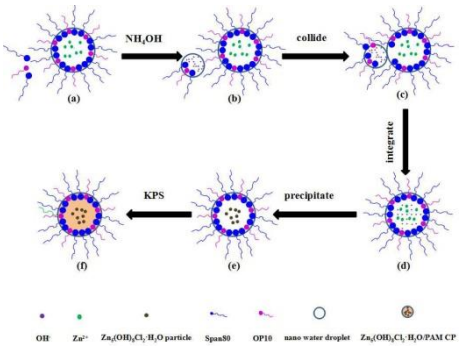

Fig. 1. Mechanism diagram of synthesis of $Zn_5(OH)_8Cl_2·H_2O$/PAM CP.

2. Experimental

2.1. Reagents

Acrylamide (AM) manufacturer was Tianjin Fu Chen chemical reagent Factory. The manufacturer of Zinc chloride, ammonia, KPS, potassium iodide, toluene was Beijing Chemical Plant. The manufacturer of Span80 and OP10 was Tianjin Huadong Reagent Factory. All reagents employed in this study were of analytical grade. They were used without further purification.

2.2. Synthesis of $Zn_5(OH)_8Cl_2·H_2O$/PAM CPs

The $Zn_5(OH)_8Cl_2·H_2O$/PAM CPs were synthesized by procedures reported in the literature [13]. At room temperature, 1.18g Span80 was added to 24mL toluene and stirred for 30 minutes to form the oil phase. 3.56g AM and 0.21g OP10 were added to 1M 5mL $ZnCl_2$ solution and stirred for 30 minutes to form the aqueous phase. At the stirring speed of 2000 rpm, the aqueous phase was slowly added to the oil phase and stirred continuously for 2h to form a stable water-in-oil

emulsion (E-1). Then the stirring speed was reduced to 1000 rpm, and 0.5mL of NH_4OH were added to the emulsion and stirred continuously for 2h to synthesize $Zn_5(OH)_8Cl_2·H_2O$ particles. After injecting the emulsion with nitrogen for 20 min, 0.05g KPS were added to initiate emulsion polymerization. The polyacrylamide was obtained for 4h. Therefore, $Zn_5(OH)_8Cl_2·H_2O$/PAM CPs were obtained in water-in-oil emulsion (E-2). The E-1 and E-2 were white emulsion. The molar ratio of $Zn_5(OH)_8Cl_2·H_2O$ to AM was 1:10.

2.3. Analytical methods

The E-1 and E-2 were placed in test tubes which were 15cm in height and 1,2 in diameter to observe the stability of them. The emulsion stability index (Vt) was equal to the volume of the remaining emulsion divided by the volume of the original emulsion of the test tube. They were tested for about 110 hours at room temperature.

The shape of $Zn_5(OH)_8Cl_2·H_2O$/PAM CPs was observed by transmission electron microscope (TEM, Hitachi H-600-II, Japan). $Zn_5(OH)_8Cl_2·H_2O$/PAM CPs were uniformly dispersed in ethanol by using ultrasound at room temperature.

Using laser particle analysis system (ZetaPlus, Brookhaven Instruments Corporation, USA), the particle size distribution and average size of $Zn_5(OH)_8Cl_2·H_2O$/PAM CPs were measured. $Zn_5(OH)_8Cl_2·H_2O$/PAM CPs were uniformly dispersed in ethanol by using ultrasound at room temperature.

X-ray powder diffraction (XRD) data were recorded by a diffractometer (Bruker D8 Discover 20kV, Cu Kα radiation).

Thermal gravimetric analysis (TGA) curves were conducted using a TGA analyzer (DTG-60H, Shimadzu, Japan) in the temperature range 25-900℃, with a heating rate of 10℃min^{-1}.

Fourier transition infrared (FT-IR) spectra were conducted using a FT-IR spectrometer (Spectrum400, PerkinElmer, USA).

Electrochemical tests were performed on the electrochemical workstation (CHI660D, Shanghai Chenhua Instrument Co., LTD., China) equipped by a three-electrode electrochemical cell consisted of a bare GCE or modified GCE as the working electrode, an Ag/AgCl (saturated potassium chloride) as the reference electrode, and platinum wire as the auxiliary electrode. The CV data were measured in 10mL of 0.1M phosphate buffer solution (PBS, pH=7.2) at scan rate of 100 mVs^{-1} and cyclic potential of +0.8-0.0V.

2.4. Preparation of $Zn_5(OH)_8Cl_2·H_2O$/PAM/GCE

The drop-coating method was used to prepare $Zn_5(OH)_8Cl_2·H_2O$/PAM/GCE. Before modification, the bare GCE was polished by 0.05μm alumina particles and then washed by deionized water and dried at room temperature. Next, 2.0μL of $Zn_5(OH)_8Cl_2·H_2O$/PAM suspension was dropped on the GCE surface. Then the solvent was evaporated at vacuum for 2 hours to obtain $Zn_5(OH)_8Cl_2·H_2O$/PAM/GCE electrode.

3. Results and discussion

The formation and dispersion of composite particles in nano water droplets very depends on the stability of emulsion [17]. According to the literature [13], when the hydrophilic-hydrophilic equilibrium (HLB) value was 5.76, the emulsion had good stability.

Therefore, we used 1.18g Span80 and 0.21g Op10 to make the HLB value of emulsion about 5.76. As shown in Fig. 2, when the HLB value was 5.76, the relationship curves between the Vt values of E-1 and E-2 and the experimental time were shown. When the time was within 18 h, the Vt value of E-1 was about 100%. As time goes on, the Vt value of E-1 decreased, and at about 110 h the Vt value was approximately 95%. That meant that E-1 was very stable. As E-2 contained $Zn_5(OH)_8Cl_2{\cdot}H_2O$/PAM CPs, the density of E-2 was greater than E1. The Vt value of E-2 showed a significant trend of decline with the increase of time. When the experimental time was about 110 h, the Vt value of E-2 was about 76%. It can be seen that E-2 had good stability.

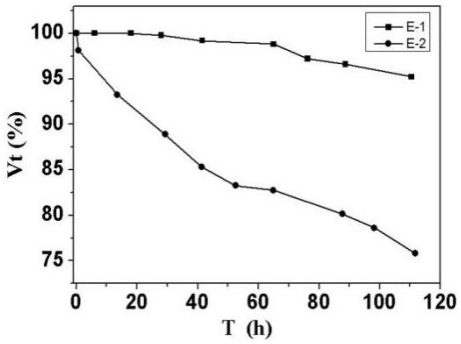

Fig. 2. The relationship curves between the Vt values of E-1 and E-2 and the experimental time (HLB=5.76).

Fig. 3 showed the XRD pattern of $Zn_5(OH)_8Cl_2{\cdot}H_2O$/PAM CPs sample. The results showed that the diffraction peaks of the sample appeared at 2θ values of 11.3°, 16.7°, 22.2°, 25.0°, 28.2°, 30.5°, 31.1°, 32.9°, 33.6°, 34.5°, 36.5°, 37.9°, 44.9°, 47.9°, 51.7°, 54.2°, 58.3° and 59.5°. These characteristic peaks were indexed to $Zn_5(OH)_8Cl_2{\cdot}H_2O$ with a rhombic hexahedral structure of (003), (101), (104), (015), (110), (113), (107), (021), (202), (018), (024), (205), (119), (125), (217), (128), (220) and (223) planes, which agreed well with $Zn_5(OH)_8Cl_2{\cdot}H_2O$ peaks (JCPDS No.07-0155). It can be determined that the sample contains $Zn_5(OH)_8Cl_2{\cdot}H_2O$.

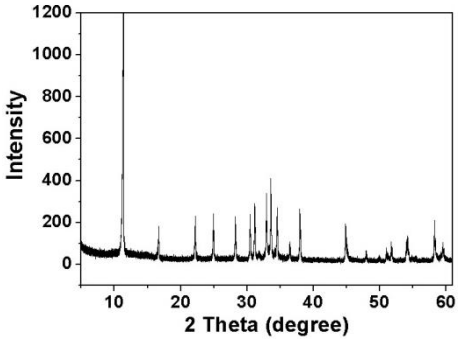

Fig. 3. XRD pattern of $Zn_5(OH)_8Cl_2{\cdot}H_2O$/PAM CPs.

Fig. 4 showed the FT-IR spectra of $Zn_5(OH)_8Cl_2{\cdot}H_2O$/PAM CPs sample. In spectra, there were the broadband near 3388 cm^{-1} and the characteristic peak at 3192 cm^{-1}. They were attributed

to the stretching vibration of N-H. The peaks at 2926 cm^{-1} and 2854 cm^{-1} were caused by C-H in the -CH_2 and -CH_3 bonds, respectively. The characteristic peaks at 1659 cm^{-1} were attributed to carbonyl stretching vibration. The stretching vibration peaks for C-N and O-C-O were located at 1453 cm^{-1} and 1102 cm^{-1} respectively. The peak at 461cm^{-1} was related to Zn-O. These characteristic peaks confirmed that $Zn_5(OH)_8Cl_2 \cdot H_2O$/PAM CPs contained Zn-O bonds and were covered by PAM.

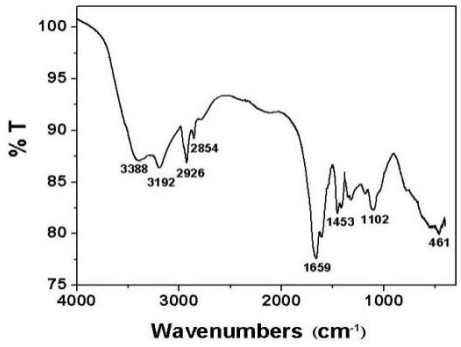

Fig. 4. FT-IR spectra of $Zn_5(OH)_8Cl_2 \cdot H_2O$/PAM CPs.

The thermal properties of $Zn_5(OH)_8Cl_2 \cdot H_2O$/PAM CPs sample were studied by TGA, as shown in Fig. 5. The weightlessness process may be divided into two stages, namely the thermal decomposition of PAM and the thermal transformation of $Zn_5(OH)_8Cl_2 \cdot H_2O$ to ZnO [18]. At about 700℃, the final total weight loss rate of the sample was 93.6%.

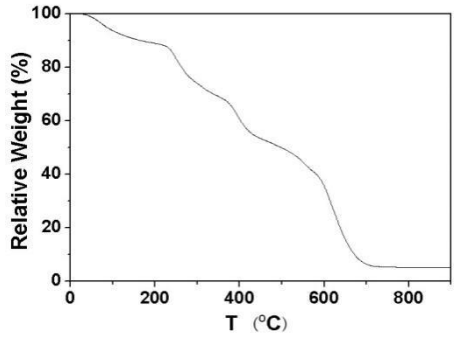

Fig. 5. TGA curve of $Zn_5(OH)_8Cl_2 \cdot H_2O$/PAM CPs.

Fig. 6 showed the TEM micrograph (A) of $Zn_5(OH)_8Cl_2 \cdot H_2O$/PAM CPs and its particle size distribution (B). As shown in Fig. 6(A), the spherical $Zn_5(OH)_8Cl_2 \cdot H_2O$/PAM CPs were uniform dispersion and had about 330-820 nm in diameter. The average diameter of $Zn_5(OH)_8Cl_2 \cdot H_2O$/PAM CPs was about 736 nm according to Fig. 6(B).

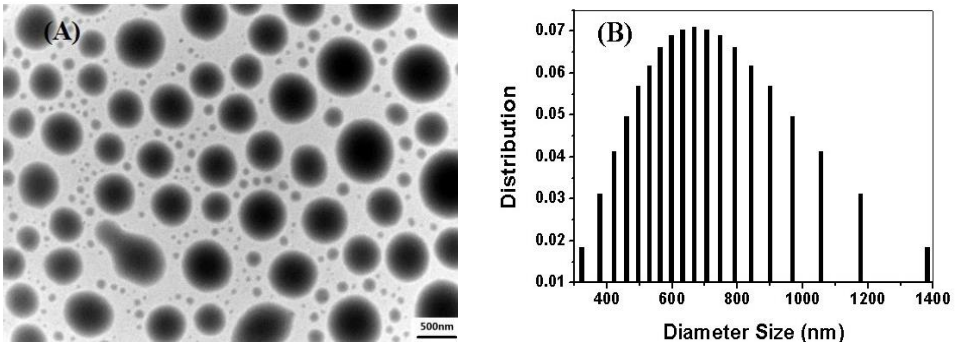

Fig. 6. (A) TEM image of $Zn_5(OH)_8Cl_2{\cdot}H_2O$/PAM CPs and (B) its particle size distribution.

Fig. 7 showed the CV curves for testing 0.01M iodide on bare GCE and $Zn_5(OH)_8Cl_2{\cdot}H_2O$/PAM/GCE respectively (scan rate: 100 mVs^{-1}, cyclic potential: +0.8-0.0V). It can be seen that bare GCE had no obvious redox peak (Fig. 7a), and $Zn_5(OH)_8Cl_2{\cdot}H_2O$/PAM/GCE had a clear redox peak (Fig. 7b) in which the anode and cathode peak voltage were 0.56V and 0.33V respectively.

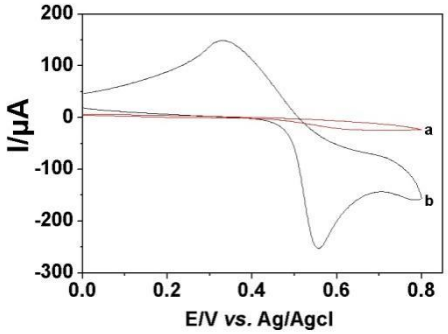

Fig. 7. The CV curves for testing 0.01M iodide on bare GCE (a) and $Zn_5(OH)_8Cl_2{\cdot}H_2O$/PAM/GCE (b). Scan rate: 100 mVs^{-1}.

The effect of various scan rates (50-400 mVs^{-1}) on the CV curves for testing 0.01M iodide on $Zn_5(OH)_8Cl_2{\cdot}H_2O$/PAM/GCE was shown in Fig. 8. It can be seen from Fig. 8(A) that the anode and cathode peak currents gradually increased with the increase of scan rate and the curves showed a quasi-reversible redox process. In Fig. 8(B), the peak current had a linear relationship with the square root of the scan rate in the scan rate range of 50-400 mVs^{-1}. It can be seen that the electrochemical reaction of iodide on $Zn_5(OH)_8Cl_2{\cdot}H_2O$/PAM/GCE belonged to diffusion control kinetics.

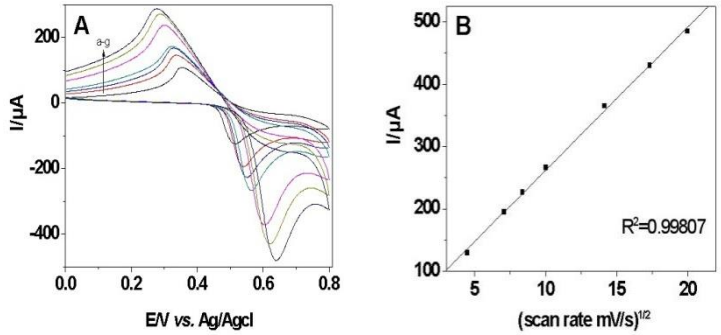

Fig. 8. (A) The CV curves for testing 0.01M iodide on $Zn_5(OH)_8Cl_2{\cdot}H_2O$/PAM/GCE. Scan rate (a-g): 20, 50, 70, 100, 200, 300, 400 mVs^{-1}. (B) plot of I vs. (scan rate)$^{1/2}$.

Fig. 9 showed the CV curves for testing iodide with various concentration (0.00001-0.01M) on $Zn_5(OH)_8Cl_2{\cdot}H_2O$/PAM/GCE (scan rate: 100 mVs^{-1}, cyclic potential: +0.8-0.0V). It can be seen that the anode and cathode peak currents rapidly increased with the increase of iodide concentration in Fig. 9(A). It indicated that the CV responses of $Zn_5(OH)_8Cl_2{\cdot}H_2O$/PAM/GCE obviously increased as iodide concentration added from 0.00001 to 0.01M. In Fig. 9(B), the CV curve for testing 0.00001M iodide on $Zn_5(OH)_8Cl_2{\cdot}H_2O$/PAM/GCE still had a clear redox peak in which the anode and cathode peak current were -18.1μA and 9.72μA respectively. Tian et al. [16] obtained similar results by coating GCE with vanadium-carbonated polypropylene. But in our CV test, the peak currents of $Zn_5(OH)_8Cl_2{\cdot}H_2O$/PAM/GCE were about ten times those obtained by Tian et al. So $Zn_5(OH)_8Cl_2{\cdot}H_2O$/PAM/GCE may be used as a sensor for detecting trace iodide.

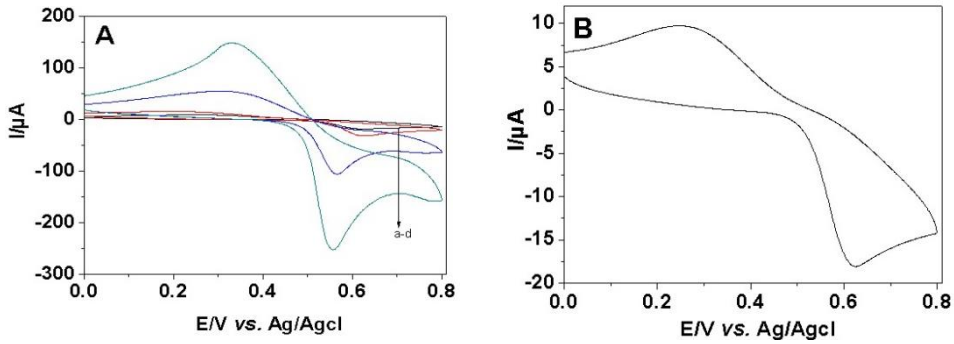

Fig. 9. (A) The CV curves for testing iodide with various concentration (a-d: 0.00001, 0.0001, 0.001, 0.01M) on $Zn_5(OH)_8Cl_2{\cdot}H_2O$/PAM/GCE and (B) the CV curve for testing 0.00001M iodide on $Zn_5(OH)_8Cl_2{\cdot}H_2O$/PAM/GCE. Scan rate: 100 mVs^{-1}.

4. Conclusions

When HLB value of 5.76, $Zn_5(OH)_8Cl_2{\cdot}H_2O$/PAM CPs were synthesized by precipitation reaction and emulsion polymerization in microreactors formed by nano water droplets. The XRD pattern showed that the CPs contained $Zn_5(OH)_8Cl_2{\cdot}H_2O$. The FT-IR characteristic peaks confirmed that the CPs contained Zn-O bonds and were covered by PAM. According to the results of TGA, the final total weight loss rate of the CPs was 93.6% at about 700℃. It can be seen from

TEM and its particle size distribution that the shape of $Zn_5(OH)_8Cl_2 \cdot H_2O$/PAM CPs were close to the spherical shape with an average diameter of about 736 nm. The CV properties for testing iodide on $Zn_5(OH)_8Cl_2 \cdot H_2O$/PAM/GCE were obtained at scan rate of 100 mVs^{-1} and cyclic potential of +0.8-0.0V. And 0.00001M iodide can be detected by $Zn_5(OH)_8Cl_2 \cdot H_2O$/PAM/GCE. In the range of 50-400mVs^{-1}, the peak current had a linear relationship with the square root of the scan rate. It can be seen that the electrochemical reaction of iodide on $Zn_5(OH)_8Cl_2 \cdot H_2O$/PAM/GCE belonged to diffusion control kinetics.

Acknowledgements

This work was supported by Daqing Normal University Scientific Research Fund (Grant No.14ZR13).

References

[1] G. G. C. Arizaga, K. G. Satyanarayana, F. Wypych, Solid. State. Ionics. **178**, 15 (2007).
[2] S. Khamlich, T. Mokrani, M. S. Dhlamini, B. M. Mothudi, M. Maaza, J. Colloid. Interf. Sci. **461**, 154 (2016).
[3] A. Moezzi, A. McDonagh, A. Dowd, M. Cortie, Inorg. Chem. **52**, 95 (2013).
[4] B. Liu, S. H. Yu, F. Zhang, L. J. Li, Q. Zhang, R. Lei, K. Jiang, J. Phys. Chem. B. **108**, 4338 (2004).
[5] X. B. Li, Y. N. Gao, X. L. Zhou, L. C. Li, L. L. Huang, J. D. Ye, T. Y. Zhang, Mater. Lett. **245**, 82 (2019).
[6] H. Tanaka, A.Fujioka, A. Futoyu, K. Kandori, T. Ishikawa, J. Solid. State. Chem. **180**, 2061 (2007).
[7] W. X. Zhang, K. Yanagisawa, Chem. Mater. **19**, 2329 (2007).
[8] J. Sithole, B. D. Ngom, S. Khamlich, E. Manikanadan, N. Manyala, Appl. Surf. Sci. **258**, 7839 (2012).
[9] D. Y. Momodu, F. Barzegar, A. Bello, J. Dangbegnon, T. Masikhwa, Electrochim. Acta **151**, 591 (**2015**).
[10] W. Zhong, P. Liu, H.G. Shi, D.S. Xue, Polym. Lett. **4**, 183 (2010).
[11] W. J. E. Beek, M. M. Wienk, R. A. J. Janssen, Adv. Mater. **16**, 1009 (2004).
[12] F. Fleischhaker, R. Zentel, Chem. Mater. **17**, 1346 (2005).
[13] Q. Y. Huang, S. Z. Wang, J. Disper. Sci. Technol. **40**, 1379 (2019).
[14] T. Fujiwara, I.U. Mohammadzai, H. Inoue, T. Kumamaru, Analyst. **125**, 759 (2000).
[15] M. P. Arena, M. D. Porter, J. S. Fritz, Anal. Chem. **74**, 185 (2002).
[16] L. Tian, L. Liu, L. Chen, N. Lu, H. D. Xu, Talanta. **66**, 130 (2005).
[17] D. Zhang, X. M. Song, F. X. Liang, Z. Y. Li, F. Q. Liu, J. Phys. Chem. B. **110**, 9079 (2006).
[18] O. Garcia-Marinez, E. Vila, R. M. Rojas, K. Petrov, J. Mater. Sci. **29**, 5429 (1994).